

Heterolytic H₂ Activation by Dihydrogen Complexes. Effects of the Ligand X in [M(X)H₂{Ph₂P(CH₂)₃PPh₂}₂]ⁿ⁺ (M = Ru, Os; X = CO, Cl, H)

Eliaana Rocchini,[†] Antonio Mezzetti,^{*,‡} Heinz Rügger,[‡] Urs Burckhardt,[‡] Volker Gramlich,[§] Alessandro Del Zotto,[†] Paolo Martinuzzi,[†] and Pierluigi Rigo[†]

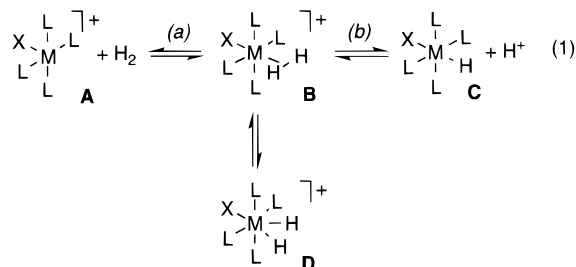
Dipartimento di Scienze e Tecnologie Chimiche, Università di Udine, Via del Cotonificio 108, I-33100 Udine, Italy, Laboratorium für Anorganische Chemie, ETH-Zentrum, CH-8092 Zürich, Switzerland, and Institut für Kristallographie und Petrographie, ETH-Zentrum, CH-8092 Zürich, Switzerland

Received May 16, 1996[®]

Complexes of the general formula [MXH₂(dppp)₂]ⁿ⁺ (M = Ru, Os; X = H, Cl, CO; dppp = 1,3-bis-(diphenylphosphino)propane) have been prepared and characterized, and the effect of the donor/acceptor properties of X on their structure and acidity has been studied. The five-coordinate complexes [MCl(dppp)₂]⁺ (M = Ru (**1a**), Os (**1b**)) react with H₂ gas in CH₂Cl₂ to give the complexes [MCl(η²-H₂)(dppp)₂]⁺ (M = Ru (**2a**), Os (**2b**)) containing elongated dihydrogen ligands. The molecular structure of **2b** has been determined by X-ray crystallography (monoclinic, space group P2₁/n with *a* = 13.314(7) Å, *b* = 18.63(2) Å, *c* = 23.20(2) Å, β = 94.58(6)°, and *Z* = 4). Chlorohydride [OsH(Cl)(dppp)₂] (**3b**) reacts with H₂ gas in the presence of Na[BPh₄] forming [OsH₃(dppp)₂]⁺ (**4b**). Protonation of [OsH₂(dppp)₂] (**5b**) with HBF₄·Et₂O also gives **4b**. A combination of X-ray crystallography (monoclinic, space group P2₁/n with *a* = 13.392(3) Å, *b* = 25.306(7) Å, *c* = 21.247(7) Å, β = 91.15(2)°, and *Z* = 4) and ¹H and ³¹P NMR studies indicate that **4b** is a classical trihydride. Hydridocarbonyls [MH(CO)(dppp)₂]⁺ (M = Ru (**6a**), Os (**6b**)) are protonated by F₃CSO₃H in CD₂Cl₂ to yield [M(CO)(η²-H₂)(dppp)₂]²⁺ (M = Ru (**7a**), Os (**7b**)), which were characterized in solution. **7a** is stable only at low temperature. Compound **7b** is a highly acidic dihydrogen complex with an estimated pK_a of −6.

Introduction

Dihydrogen complexes allow for the design of a simple, fascinating pathway for the heterolytic activation of molecular hydrogen by means of transition metal compounds. The overall process can be sketched according to eq 1 as (a) the formation of dihydrogen complex **B** (or of the classical hydride **D**) by addition of H₂ to the coordinatively unsaturated metal fragment **A**, followed by (b) dissociation of H⁺ to give monohydride **C**.



Crabtree and Lavin have recognized at an early stage that dihydrogen complexes can act as Brønsted acids.¹ This has led to systematic investigations of ligand effects and to the discovery of highly acidic dihydrogen complexes.² Although conclusive experimental evidence is still lacking, the reaction sequence **A** → **B** → **C** is thought to play a key role in some homogeneous

hydrogenation reactions.^{2a,3} The Brønsted acidity of **B** can be expected to be of fundamental importance for stoichiometric and catalytic hydrogenations which are sensitive to the concentration of acid.⁴

The reactivity of formally unsaturated transition metal complexes with H₂ was first reported for [M(CO)₃(η²-H₂)L₂] (M = Cr, Mo, W; L = phosphine)^{2a,b} and, more recently, for [Re(CO)₃(η²-H₂)L₂]⁺.⁵ Agostic interactions stabilize the unsaturated, 16-electron fragments [M(CO)₃L₂]ⁿ⁺ (*n* = 0 or 1). A further stabilization mechanism for the five-coordinate fragment **A** has been suggested recently for the case in which X is a π-donor.⁶ Thus, when one hydride ligand is substituted by halide in RuH₅L₂ and IrH₅L₂, the (formally) 16-electron species Ru(X)H(η²-H₂)L₂ (X = Cl, I)^{7a} and Ir(Cl)H₂L₂^{7b} are stabilized by X → M π-donation. Reversing this argument suggests that “π-stabilized unsaturated compounds may readily bind H₂, and some of them might be dihydrogen compounds”.^{6b} Actually, five-coordinate complexes of the type [MCl(L₂)₂]ⁿ⁺ (M = Ru or Os, L₂ = diphosphine ligand)^{8,9,c} have been known to react with molecular hydrogen to give *trans*-[MCl(η²-H₂)(L₂)₂]ⁿ⁺, which contain an elongated dihydrogen ligand.⁹

[†] Università di Udine.

[‡] Laboratorium für Anorganische Chemie.

[§] Institut für Kristallographie und Petrographie.

[®] Abstract published in *Advance ACS Abstracts*, January 1, 1997.

- (1) Crabtree, R. H.; Lavin, M. *J. Chem. Soc., Chem. Commun.* **1985**, 794.
- (2) (a) Jessop, P. G.; Morris, R. H. *Coord. Chem. Rev.* **1992**, *121*, 155. (b) Heinekey, D. M.; Oldham, W. J. *Chem. Rev.* **1993**, *93*, 913. (c) Morris, R. H. *Inorg. Chem.* **1992**, *31*, 1471. (d) Schlaf, M.; Lough, A. J.; Morris, R. H. *Organometallics* **1993**, *12*, 3808. (e) Schlaf, M.; Lough, A. J.; Maltby, P. A.; Morris, R. H. *Organometallics* **1996**, *15*, 2270. (f) Heinekey, D. M.; Luther, T. A. *Inorg. Chem.* **1996**, *35*, 4396.

- (3) (a) Crabtree, R. H. *The Organometallic Chemistry of the Transition Metals*; Wiley: New York, 1988; p 198. (b) Ashby, M. T.; Halpern, J. *J. Am. Chem. Soc.* **1991**, *113*, 589.

- (4) See, for instance: (a) Bullock, R. M.; Song, J.-S.; Szalda, D. J. *Organometallics* **1996**, *15*, 2504. (b) Mezzetti, A.; Tschumper, A.; Consiglio, G. *J. Chem. Soc., Dalton Trans.* **1995**, 49 and references therein.

- (5) Heinekey, D. M.; Schomber, B. M.; Radzewich, C. E. *J. Am. Chem. Soc.* **1994**, *116*, 4515.

- (6) (a) Caulton, K. G. *New J. Chem.* **1994**, *18*, 25. (b) Johnson, T. J.; Folting, K.; Streib, W. E.; Martin, J. D.; Huffman, J. C.; Jackson, S. A.; Eisenstein, O.; Caulton, K. G. *Inorg. Chem.* **1995**, *34*, 488. (c) Riehl, J.-F.; Jean, Y.; Eisenstein, O.; Péliissier, M. *Organometallics* **1992**, *11*, 729.

- (7) (a) Chaudret, B.; Chung, G.; Eisenstein, O.; Jackson, S. A.; Lahoz, F. J.; Lopez, J. A. *J. Am. Chem. Soc.* **1991**, *113*, 2314. (b) Mediati, M.; Tachibana, G. N.; Jensen, C. M. *Inorg. Chem.* **1992**, *31*, 1827.

With minor exceptions,¹⁰ X is either H or Cl in most dihydrogen complexes of the type $\text{trans}[\text{MX}(\eta^2\text{-H}_2)\text{L}_4]^+$ (M = d⁶ metal ion, L = phosphine ligand). However, a thorough investigation of the related system $\text{trans}[\text{OsL}(\eta^2\text{-H}_2)(\text{en})_2]^{n+}$ (en = 1,2-diaminoethane), with L chosen amongst a wide variety of neutral and anionic ligands, has shown that the *trans* ligand L deeply affects the H–H distance.¹¹ Thus, we became intrigued by the question of whether it is possible to choose an ancillary ligand X which both stabilizes the five-coordinate species **A** and imparts a high Brønsted acidity to the dihydrogen complex **B**, in order to achieve the reaction sequence **A** → **B** → **C** in eq 1.

Since only $[\text{RuH}(\eta^2\text{-H}_2)(\text{dppp})_2]^+$ has been reported in the dppp series,¹² we prepared the dihydrogen complexes $[\text{MX}(\eta^2\text{-H}_2)(\text{dppp})_2]^+$ (M = Ru or Os, dppp = 1,3-bis(diphenylphosphino)propane) with different X ligands and measured their Brønsted acidity. The reaction of the previously reported five-coordinate complexes $[\text{MCl}(\text{dppp})_2]^+$ (M = Ru (**1a**), Os (**1b**))^{8a,b} with H₂ gave dihydrogen complexes containing chloride, a π -donor. Then, X was changed to hydride (a strong σ -donor) and to a strong π -acceptor, such as carbon monoxide. Protonation of the monohydrides **C** was used for the synthesis of dihydrogen complexes containing CO. The first results of this investigation are reported in the present paper.

Experimental Section

General Considerations. All manipulations involving solutions of the complexes were performed under argon with use of Schlenk line techniques. Solvents were purified by standard methods. All chemicals used were of reagent grade or comparable purity. The ligand dppp, $\text{RuCl}_3 \cdot \text{H}_2\text{O}$, and $(\text{NH}_4)_2\text{OsCl}_6$ were purchased from Aldrich; $\text{RuCl}_2 \cdot (\text{PPh}_3)_3$,¹³ $[\text{RuH}(\text{Cl})(\text{dppp})_2]$,¹⁴ and $[\text{RuH}(\eta^2\text{-H}_2)(\text{dppp})_2][\text{PF}_6]^{12a} were prepared according to the literature. Yields are based on the metal. Infrared spectra were recorded on a Nicolet Magna 550 FT-IR spectrophotometer. Microanalyses were performed by the Microanalytical Laboratory of the Dipartimento di Scienze e Tecnologie Chimiche, Università di Udine. ¹H and ³¹P{¹H} NMR spectra were obtained with Bruker AMX 500 or AC 200 spectrometers; solid state ³¹P{¹H} CP-MAS NMR spectra were recorded on a Bruker AMX 400. ³¹P chemical shifts are relative to 85% H₃PO₄ and (NH₄)₂H₂PO₄ for solutions and solids, respectively. Inverse-gated decoupling was used to record the ³¹P NMR spectra when their integration was required. Spectral simulations were performed with PANIC (Bruker Spectrospin AG). Low-temperature ³¹P NMR data are reported in Table 1, and selected ¹H NMR data (*T*₁(min) and *J*(D,H)) in Table 2.$

- (8) (a) Bressan, M.; Rigo, P. *Inorg. Chem.* **1975**, *14*, 2286. (b) Bressan, M.; Ettore, R.; Rigo, P. *Inorg. Chim. Acta* **1977**, *24*, L57. (c) Batista, A. A.; Centeno Cordeiro, L. A.; Oliva, G. *Inorg. Chim. Acta* **1993**, *203*, 185. (d) Mezzetti, A.; Del Zotto, A.; Rigo, P.; Bresciani Pahor, N. *J. Chem. Soc., Dalton Trans.* **1989**, 1045. (e) Mezzetti, A.; Del Zotto, A.; Rigo, P. *J. Chem. Soc., Dalton Trans.* **1990**, 2515.
- (9) (a) Cappellani, E. P.; Maltby, P. A.; Morris, R. H.; Schweitzer, C. T.; Steele, M. R. *Inorg. Chem.* **1989**, *28*, 4437. (b) Mezzetti, A.; Del Zotto, A.; Rigo, P.; Farnetti, E. *J. Chem. Soc., Dalton Trans.* **1991**, 1525. (c) Burrell, A. K.; Bryan, J. C.; Kubas, G. J. *J. Am. Chem. Soc.* **1994**, *116*, 1575. (d) Chin, B.; Lough, A. J.; Morris, R. H.; Schweitzer, C. T.; D'Agostino, C. *Inorg. Chem.* **1994**, *33*, 6278. (e) Maltby, P. A.; Schlaf, M.; Steinbeck, M.; Lough, A. J.; Morris, R. H.; Klooster, W. T.; Koetzle, T. F.; Srivastava, R. C. *J. Am. Chem. Soc.* **1996**, *118*, 5396.
- (10) Jiménez-Tenorio, M.; Puerta, M. C.; Valerga, P. *J. Chem. Soc., Chem. Commun.* **1993**, 1750.
- (11) (a) Li, Z.-W.; Taube, H. *J. Am. Chem. Soc.* **1991**, *113*, 8946. (b) Hasegawa, T.; Li, Z.-W.; Parkin, S.; Hope, H.; McMullan, R. K.; Koetzle, T. F.; Taube, H. *J. Am. Chem. Soc.* **1992**, *114*, 2712. (c) Li, Z.-W.; Taube, H. *J. Am. Chem. Soc.* **1994**, *116*, 4352.
- (12) (a) Ashworth, T. V.; Singleton, E. *J. Chem. Soc., Chem. Commun.* **1976**, 705. (b) Saburi, M.; Aoyagi, K.; Takahashi, T.; Uchida, Y. *Chem. Lett.* **1990**, 601.
- (13) Stephenson, T. A.; Wilkinson, G. *J. Inorg. Nucl. Chem.* **1966**, *28*, 945.
- (14) James, B. R.; Wang, D. K. W. *Inorg. Chim. Acta* **1976**, *19*, L17.

Table 1. Low-temperature ³¹P NMR Data^a

	δ (ppm)	² <i>J</i> (P,P') (Hz)	T (K)
2a	−4.1 (t), 18.5 (t)	31.6	183
2b	−42.5 (t), −16.6 (t)	22.3	193
3a^b	10.3 (t), 25.5 (t)	41.3	173
3b	−27.9 (t), −14.9 (t)	29.5	173
4b	3.3 (t), −25.2 (t)	22.6	193
6a	15.3 (t), 20.5 (t)	35.9	173
6b	−23.4 (t), −19.6 (t)	24.9	173
7a	3.7 (t), 12.3 (t)	24.6	173
7b	−32.3 (t), −22.1 (t)	17.9	173

^a In CD₂Cl₂ solution. ^b ¹H NMR (CD₂Cl₂, 173 K, 200 MHz): δ −17.5 (tt, 1 H, RuH, *J*(P,H) = 25.4, *J*(P',H) = 12.7 Hz).

Table 2. ¹H NMR Data for $[\text{MXH}_2(\text{dppp})_2]^{n+}$ ^a

	X	<i>T</i> ₁ (min) (ms)	<i>d</i> (H–H) (Å) ^b	<i>J</i> (D,H) (Hz) ^c	<i>J</i> (P,H) (Hz)	T (K)
2a	Cl	8.2	1.0	24 ^d	8	223
2b	Cl	23.7	1.2	11	11	213
4a	H	5.5 ^e	0.89	32		243
4b	H	72	1.6 ^f	0	g	243
7a	CO	5.0	0.85	34 ^h		223
7b	CO	5.5	0.89	32		233

^a CD₂Cl₂ solution, 200 MHz. ^b Calculated using eq 6.^{9e} ^c At room temperature, unless otherwise stated. ^d Measured at 0 °C. ^e Literature value: 6 ms at 400 MHz.^{8b} ^f Nonbonded distance. ^g See text. ^h Measured at −80 °C.

Preparation of $[\text{RuCl}(\text{dppp})_2][\text{PF}_6]$ (1a**).** An improved procedure consisted of refluxing $[\text{RuCl}_2(\text{PPh}_3)_3]$ (1.00 g, 1.04 mmol), dppp (0.86 g, 2.09 mmol), and NH₄[PF₆] (0.51 g, 3.1 mmol) in 30 mL of EtOH for 4 h. Recrystallization from CH₂Cl₂/PrOH gave brown microcrystals with properties consistent with those reported in the literature.^{8a} Yield: 1.00 g, 87%. ¹H NMR (CD₂Cl₂, 200 MHz, 293 K): δ 8.0–6.9 (m, PC₆H₅), 2.6 (br, 4 H, PCH₂), 2.2 (br, 4 H, PCH₂), 1.7 (br, 4 H, PCH₂CH₂). ³¹P{¹H} NMR (CD₂Cl₂, 81 MHz, 293 K): δ −1.6 (t), 43.2 (t, *J*(P,P') = 31.5 Hz), −143.9 (sept, *J*(P,F) = 711 Hz).

Preparation of $[\text{OsCl}(\text{dppp})_2][\text{PF}_6]$ (1b**).** An improved procedure consisted of refluxing (NH₄)₂OsCl₆ (1.00 g, 2.28 mmol) and dppp (3.30 g, 8.00 mmol) in 50 mL of CH₃O(CH₂)₂OH for 6 h. After the solution was cooled, NH₄[PF₆] (1.12 g, 6.84 mmol) in 20 mL of EtOH was added thereto. The brown precipitate was filtered off, vacuum dried, and recrystallized from CH₂Cl₂/PrOH. Yield: 1.75 g, 65%. Anal. Calcd for C₅₄H₅₂ClF₆OsP₃: C, 54.25; H, 4.38. Found: C, 55.06; H, 4.54. Physical properties consistent with those reported in the literature.^{8b} ¹H NMR (CD₂Cl₂, 200 MHz, 293 K): δ 8.0–6.8 (m, PC₆H₅), 2.9 (br, 4 H, PCH₂), 2.4 (br, 4 H, PCH₂), 1.6 (br, 4 H, PCH₂CH₂). ³¹P{¹H} NMR (CD₂Cl₂, 81 MHz, 293 K): δ −23.0 (t), −17.5 (t, *J*(P,P') = 16.7 Hz), −143.9 (sept, *J*(P,F) = 711 Hz).

Reaction of **1a with H₂ at Low Pressure.** $[\text{RuCl}(\text{dppp})_2][\text{PF}_6]$ (25 mg, 0.045 mmol) was dissolved in 0.25 mL of CD₂Cl₂ in a Wilmad NMR tube fitted with a pressure valve. The tube was connected alternatively to a high vacuum or hydrogen by means of a manifold and Swagelok fittings, and after three freeze–pump–thaw cycles, the tube was filled with hydrogen. Two distinct experiments were run with a H₂ pressure of 1 and 2 atm. After the valve was closed, the tube was rapidly warmed to room temperature and transferred into the NMR magnet (*T* = 23 °C). ¹H and inverse-gated {¹H}-decoupled ³¹P NMR spectra were recorded over a period of 96 h. The H₂ concentration has been corrected for 25% NMR-silent parahydrogen.

Observation of $\text{trans}[\text{RuCl}(\eta^2\text{-H}_2)(\text{dppp})_2][\text{PF}_6]$ (2a**).** Complex **1a** (50 mg, 0.090 mmol) was dissolved in 0.5 mL of CD₂Cl₂ in an NMR tube and transferred into a stainless steel autoclave, which was closed, purged with H₂ (50 atm), and pressurized to 300 atm. After 36 h at room temperature, the pressure was released. The sample, whose color had turned pale yellow, was removed from the autoclave and was immediately frozen in liquid nitrogen. Afterward, the sample was kept at −25 °C. ¹H NMR (CD₂Cl₂, 200 MHz, 293 K): δ 8.0–6.9 (m, PC₆H₅), 2.8 (br, 4 H, PCH₂), 2.2 (br, 4 H, PCH₂), 1.7 (br, 4 H, PCH₂CH₂), −10.6 (br, 2 H, RuH₂). ³¹P{¹H} NMR (CD₂Cl₂, 81 MHz, 293 K): δ 6.6 (br), −143.9 (sept, *J*(P,F) = 711 Hz).

Table 3. Selected Bond Distances (Å) and Angles (deg) for [OsCl(η^2 -H₂)(dppp)₂][PF₆]

Os(1)–Cl(1)	2.437(4)	Os(1)–P(3)	2.412(4)
Os(1)–P(1)	2.416(4)	Os(1)–P(4)	2.416(4)
Os(1)–P(2)	2.428(4)		
Cl(1)–Os(1)–P(1)	84.1(1)	P(2)–Os(1)–P(3)	96.1(1)
Cl(1)–Os(1)–P(2)	93.4(1)	Cl(1)–Os(1)–P(4)	97.7(1)
P(1)–Os(1)–P(2)	86.8(1)	P(1)–Os(1)–P(4)	93.4(1)
Cl(1)–Os(1)–P(3)	84.5(1)	P(2)–Os(1)–P(4)	168.9(1)
P(1)–Os(1)–P(3)	168.4(1)	P(3)–Os(1)–P(4)	85.9(1)

Preparation of *trans*-[OsCl(η^2 -H₂)(dppp)₂][PF₆] (2b). [OsCl(dppp)₂][PF₆] (1.0 g, 0.84 mmol) was dissolved in 30 mL of CH₂Cl₂ under hydrogen. The solution turned colorless within 2 h. Addition of 40 mL of ⁱPrOH, followed by partial evaporation of the solution, yielded a white product, which was filtered off and vacuum dried. The ¹H NMR spectrum indicates that the microcrystalline product contains 1 molecule of ⁱPrOH per mole of complex. Yield: 0.89 g, 84%. Anal. Calcd for C₅₇H₆₂ClF₆OOSp₅: C, 54.44; H, 4.97. Found: C, 54.04; H, 5.01. ¹H NMR (CD₂Cl₂, 200 MHz, 293 K): δ 7.6–6.9 (m, PC₆H₅), 3.1 (br, 4 H, PCH₂), 2.4 (br, 4 H, PCH₂), 1.6 (br, 4 H, PCH₂CH₂), –10.0 (br, 2 H, OsH₂). ³¹P{¹H} NMR (CD₂Cl₂, 81 MHz, 293 K): δ –30.0 (br), –143.9 (sept, J(P,F) = 711 Hz).

X-ray Structure Analysis of [OsCl(η^2 -H₂)(dppp)₂][PF₆] (2b). Colorless crystals of **2b** suitable for X-ray analysis were obtained from CH₂Cl₂/ⁱPrOH. Crystal data for C₅₄H₅₄ClF₆OOSp₅·2CH₂Cl₂ (fw = 1365.3): monoclinic, space group *P*2₁/*n*, cell dimensions at 293 K are *a* = 13.314(7) Å, *b* = 18.63(2) Å, *c* = 23.20(2) Å, β = 94.58(6)°, and *V* = 5735(9) Å³ with *Z* = 4 and *D*_{calcd} = 1.581 Mg/m³, μ (Mo K α) = 26.52 cm^{–1} (graphite monochromated), λ = 0.710 73 Å, and *F*(000) = 2728. The data were collected on a Syntex P21 diffractometer using the ω scan mode (2 θ range = 3.0–40.0°) with variable scan speeds (1.0–4.0°/min in ω) to ensure constant statistical precision on the collected intensities. No absorption correction was applied. The structure was solved using Patterson methods. Of the 4965 independent reflections with the index ranges $-12 \leq h \leq 8$, $0 \leq k \leq 17$, and $0 \leq l \leq 22$, 3982 with *F* > 4.0 σ (*F*) were used in the refinement. A total of 653 parameters were refined by full-matrix least-squares using SHELXTL PLUS (data-to-parameter ratio 6.1:1, quantity minimized $\Sigma w(F_o - F_c)^2$), with anisotropic displacement parameters for all non-H atoms. The contribution of the H atoms in idealized positions (riding model with fixed isotropic *U* = 0.080 Å²) was taken into account but not refined. Two independent CH₂Cl₂ molecules were located in the final Fourier map. Final residuals (observed data) were *R* = 0.053 and *R*_w = 0.070, goodness-of-fit (GOF) = 0.98 (weighting scheme $w^{-1} = \sigma^2(F) + 0.0050 F^2$). Maximum and minimum difference peaks were 2.29 and –1.26 eÅ^{–3}, respectively, largest and mean Δ/σ = 0.306 and 0.028. Tables of atomic coordinates, anisotropic displacement coefficients, and an extended list of interatomic distances and angles are available as Supporting Information. Selected bond distances and angles are reported in Table 3.

Preparation of [OsH(Cl)(dppp)₂] (3b). *trans*-[OsCl(η^2 -H₂)(dppp)₂][PF₆] (0.80 g, 0.67 mmol) and EtONa (46 mg, 0.67 mmol) were suspended in 20 mL of acetone. After the solution was stirred at room temperature for 2 h, the pale yellow product was filtered off, washed with acetone, and vacuum dried. Recrystallization was from CH₂Cl₂/hexane. Yield: 0.64 g, 90%. Anal. Calcd for C₅₄H₅₃ClOsp₄: C, 61.68; H, 5.08. Found: C, 60.87; H, 5.01. IR (Nujol), cm^{–1}: ν (OsH) 2117 (s). ¹H NMR (CD₂Cl₂, 200 MHz, 293 K): δ 7.5–6.8 (m, PC₆H₅), 2.9 (br, 4 H, PCH₂), 2.4 (br, 4 H, PCH₂), 1.5 (br, 4 H, PCH₂CH₂), –20.0 (quintet, 1 H, OsH, *J*(P,H) = 15.5 Hz). ¹H NMR (CD₂Cl₂, 200 MHz, 173 K): δ –19.7 (tt, 1 H, OsH, *J*(P,H) = 17.8, *J*(P',H) = 8.9 Hz). ³¹P{¹H} NMR (CD₂Cl₂, 81 MHz, 293 K): δ –21.9 (br).

Preparation of [OsH₃(dppp)₂][BPh₄] (4b·BPh₄). Na[BPh₄] (146 mg, 0.43 mmol) in 5 mL of EtOH was added to [OsH(Cl)(dppp)₂] (0.30 g, 0.29 mmol) in 20 mL of CH₂Cl₂. After the solution was stirred under H₂ (1 atm) at room temperature for 1 h, 5 mL of EtOH were added. Concentration of the solution yielded a white precipitate, which was filtered off, washed with EtOH, and vacuum dried. Recrystallization was from CH₂Cl₂/ⁱPrOH. Anal. Calcd for C₇₈H₇₃BOsP₄: C, 70.05; H, 5.65. Found: C, 69.46; H, 5.61. IR (Nujol), cm^{–1}: ν (OsH₃) 1994 (s). ¹H NMR (CD₂Cl₂, 200 MHz, 293 K): δ 7.4–6.8 (m, PC₆H₅),

Table 4. Selected Bond Distances (Å) and Angles (deg) for [OsH₃(dppp)₂][PF₆]

Os(1)–P(1)	2.379(4)	Os(1)–P(3)	2.375(4)
Os(1)–P(2)	2.356(4)	Os(1)–P(4)	2.358(4)
P(1)–Os(1)–P(2)	87.6(1)	P(1)–Os(1)–P(4)	95.6(1)
P(1)–Os(1)–P(3)	136.6(1)	P(2)–Os(1)–P(4)	169.1(1)
P(2)–Os(1)–P(3)	97.3(1)	P(3)–Os(1)–P(4)	87.6(1)

2.5 (br, 8 H, PCH₂), 1.7 (br, 4 H, PCH₂CH₂), –6.4 (br quintet, 3 H, OsH₃, *J*(P,H) = 8.4 Hz). ¹H NMR (CD₂Cl₂, 200 MHz, 193 K): δ –6.10 (BB' of BB'XX'YY', OsH_{B2}, 2 H, *J*(P,H) = 13.6, *J*(P,H) + *J*(P',H) = 12.8 Hz), –7.41 (A of AXX'YY', tt, OsH_A, 1 H, OsH, *J*(P,H) = 32.0, *J*(P',H) = 7.0 Hz). ³¹P{¹H} NMR (CD₂Cl₂, 81 MHz, 293 K): δ –12.9 (br).

X-ray Structure Analysis of [OsH₃(dppp)₂][BPh₄] (4b·BPh₄). Colorless crystals of **4b·BPh₄** suitable for X-ray analysis were obtained from CH₂Cl₂/ⁱPrOH. Crystal data for C₇₈H₇₃BOsP₄·2CH₂Cl₂ (fw 1504.1): monoclinic, space group *P*2₁/*n*, with cell dimensions at 293 K of *a* = 13.392(3) Å, *b* = 25.306(7) Å, *c* = 21.247(7) Å, β = 91.15–(2)°, and *V* = 7199(3) Å³ with *Z* = 4 and *D*_{calcd} = 1.388 Mg/m³, μ (Mo K α) = 20.52 cm^{–1} (graphite monochromated), λ = 0.710 73 Å, and *F*(000) = 3060. The data were collected on a Syntex P21 diffractometer using the ω scan mode (2 θ range = 3.0–40.0°). Data collection was as described above for **2b**. No absorption correction was applied. The structure was solved using Patterson methods. Of the 3691 independent reflections with the index ranges $0 \leq h \leq 12$, $-24 \leq k \leq 24$, and $-20 \leq l \leq 0$, 2638 with *F* > 3.0 σ (*F*) were used in the refinement. A total of 543 parameters were refined by full-matrix least-squares using SHELXTL PLUS (data-to-parameter ratio 4.9:1, quantity minimized $\Sigma w(F_o - F_c)^2$). All phenyl rings were refined as rigid groups. For non-H atoms, anisotropic displacement parameters were applied, except for [BPh₄][–] which was refined isotropically. The contribution of the H atoms in idealized positions (riding model with fixed isotropic *U* = 0.080 Å²) was taken into account but not refined. Two independent CH₂Cl₂ molecules were located in the final Fourier map. Final residuals (observed data) were *R* = 0.034 and *R*_w = 0.040, GOF = 0.69 (weighting scheme $w^{-1} = \sigma^2(F) + 0.0019 F^2$) with maximum and minimum difference peaks of 0.38 and –0.37 eÅ^{–3}, respectively, largest and mean Δ/σ = 0.715 and 0.055. Tables of atomic coordinates, anisotropic displacement coefficients, and extended lists of interatomic distances and angles are available as Supporting Information. Selected bond distances and angles are reported in Table 4.

Preparation of *cis*-[OsH₂(dppp)₂] (5b). [OsCl(dppp)₂][PF₆] (0.41 g, 0.34 mmol) and EtONa (47 mg, 0.68 mmol) were dissolved in 20 mL of CH₂Cl₂ and stirred overnight at room temperature under H₂ (1 atm). Addition of 20 mL of hexane and concentration of the solution gave a white precipitate. Yield: 0.26 g, 75%. Recrystallization was from CH₂Cl₂/hexane. Anal. Calcd for C₅₄H₅₄Osp₄: C, 63.77; H, 5.35. Found: C, 63.25; H, 5.36. IR (Nujol), cm^{–1}: ν (OsH₂) 1986, 1957 (s). ¹H NMR (CD₂Cl₂, 200 MHz, 293 K): δ 8.2–6.6 (m, PC₆H₅), 2.9–2.3 (br, 8 H, PCH₂), 2.0 (br, 4 H, PCH₂CH₂), –9.24 (m, 2 H, OsH₂). ³¹P{¹H} NMR (CD₂Cl₂, 81 MHz, 293 K): δ –9.4 (AA' of AA'BB'), –10.4 (BB' of AA'BB', *J*(A,B) = 18.6, *J*(A,B') = 18.4, *J*(B,B') = 21.7, *J*(A,A') (trans) not refined).

Preparation of [OsH₃(dppp)₂][BF₄] (4b·BF₄). A C₆H₆ solution (30 mL) of *cis*-[OsH₂(dppp)₂] (0.40 g, 0.39 mmol) was treated with 85% HBF₄·Et₂O (70 μ L, 0.40 mmol). A white precipitate was formed, which was filtered off and vacuum dried. Yield: 350 mg, 81%. Anal. Calcd for C₅₄H₅₃BF₄Osp₄: C, 58.70; H, 5.02. Found: C, 57.93; H, 4.96. Spectroscopic data were as given above.

Preparation of [RuH(CO)(dppp)₂][BPh₄] (6a). Na[BPh₄] (62 mg, 0.18 mmol) in 5 mL of EtOH was added to [RuH(Cl)(dppp)₂] (0.17 g, 0.18 mmol) in 20 mL of CH₂Cl₂. After the solution was stirred under CO (1 atm) at room temperature for 1 h, 20 mL of ⁱPrOH were added. Concentration of the solution yielded a white precipitate, which was filtered off, washed with ⁱPrOH, and vacuum dried. Recrystallization was from CH₂Cl₂/ⁱPrOH. Yield: 184 mg, 80%. Anal. Calcd for C₇₉H₇₃BOP₄Ru: C, 74.47; H, 5.77. Found: C, 74.10; H, 5.73. IR (CH₂Cl₂), cm^{–1}: ν (CO) 1978 (s), ν (RuH) 2057 (s). ¹H NMR (CD₂Cl₂, 200 MHz, 293 K): δ 7.8–6.7 (m, PC₆H₅), 2.3 (br, 4 H, PCH₂),

Table 5. Estimated pK_a Values^a

	K_{eq}	pK_a	base
2a	0.020 ± 0.006	4.4	PPh ₃
2b	0.022 ± 0.008	12.5	NEt ₃
4a	4.6 ± 0.8	10.2	NEt ₃
4b	3.5 ± 1.2	10.3	NEt ₃
7a	<i>b</i>	ca. -6	CF ₃ SO ₃ ⁻
7b	5.8 ± 1.7	-5.7	CF ₃ SO ₃ ⁻

^a On the pseudo-aqueous scale, see eqs 4 and 5. K_{eq} values reported with standard errors. ^b Not determined.

2.0 (br, 4 H, PCH₂), 1.6 (br, 4 H, PCH₂CH₂), -5.1 (quintet, 1 H, RuH, $J(P,H)$ = 20.4 Hz). ¹H NMR (CD₂Cl₂, 200 MHz, 173 K): δ -5.2 (tt, 1 H, RuH, $J(P,H)$ = 26.8, $J(P',H)$ = 13.5 Hz). ³¹P{¹H} NMR (CD₂Cl₂, 81 MHz, 293 K): δ 18.1 (br s).

Preparation of [OsH(CO)(dppp)₂][BPh₄] (6b**).** Na[BPh₄] (65 mg, 0.19 mmol) and [OsH(Cl)(dppp)₂] (0.20 g, 0.19 mmol) were treated as given for **6a**. The crude reaction product refluxed in CH₃OH for 8 h gave the pure *trans* isomer. Yield: 200 mg, 77%. Anal. Calcd for C₇₉H₇₃BOOsP₄: C, 69.60; H, 5.40. Found: C, 69.12; H, 5.37. IR (CH₂Cl₂), cm⁻¹: ν (CO) 1972 (s), ν (RuH) 2055 (s). ¹H NMR (CD₂Cl₂, 200 MHz, 293 K): δ 7.9–6.7 (m, PC₆H₅), 2.6 (br, 4 H, PCH₂), 2.2 (br, 4 H, PCH₂), 1.5 (br, 4 H, PCH₂CH₂), -6.1 (quintet, 1 H, OsH, $J(P,H)$ = 19.2 Hz). ¹H NMR (CD₂Cl₂, 200 MHz, 173 K): δ -6.3 (tt, 1 H, OsH, $J(P,H)$ = 24.5, $J(P',H)$ = 12.5 Hz). ³¹P{¹H} NMR (CD₂Cl₂, 81 MHz, 293 K): δ -21.8 (br s).

Observation of [Ru(CO)(η^2 -H₂)(dppp)₂]²⁺ (7a**).** *trans*-[RuH(CO)(dppp)₂][BPh₄] (20 mg, 16 μ mol) was dissolved in 0.5 mL of CD₂Cl₂ under argon in an NMR tube; the solution was cooled to -40 °C, and CF₃SO₃H (20 μ L, 0.23 mmol) was added thereto by means of a syringe. ¹H NMR (CD₂Cl₂, 200 MHz, 243 K): δ 9.1–6.5 (m, PC₆H₅), 2.5 (br, 8 H, PCH₂), 1.5 (br, 4 H, PCH₂CH₂), -2.5 (br, 2 H, RuH₂). ³¹P{¹H} NMR (CD₂Cl₂, 81 MHz, 243 K): δ 7.6 (br s).

Observation of [Os(CO)(η^2 -H₂)(dppp)₂]²⁺ (7b**).** *trans*-[OsH(CO)(dppp)₂][BPh₄] (20 mg, 15 μ mol) was dissolved in 0.5 mL of CD₂Cl₂ under argon in an NMR tube, and CF₃SO₃H (20 μ L, 0.23 mmol) was added thereto by means of a syringe. ¹H NMR (CD₂Cl₂, 200 MHz, 293 K): δ 8.0–6.6 (m, PC₆H₅), 2.8 (br, 8 H, PCH₂), 2.0 (br, 4 H, PCH₂CH₂), -3.0 (br, 2 H, OsH₂). ³¹P{¹H} NMR (CD₂Cl₂, 81 MHz, 293 K): δ -29.7 (br s).

Acidity Measurements. The equilibrium constant K_{eq} of reaction (4) was measured by ³¹P and ¹H NMR in CD₂Cl₂ for all η^2 -H₂ complexes, with the exception of **7a**. The solvent was dried over molecular sieves and saturated with argon or H₂ before use. The concentrations of [M(H)X(dppp)₂] and [MX(η^2 -H₂)(dppp)₂]⁺ were obtained by integration of the inverse-gated decoupled ³¹P spectra recorded at 293 K and checked by integration of the ¹H NMR spectra (hydride part). At least three measurements were performed for each complex. Details of the calculation of the equilibrium constants K_{eq} are given below. The K_{eq} values are reported in Table 5, together with their standard errors and with pK_a values that were estimated assuming pK_a (NH₃⁺) = 10.8,^{2a} pK_a (Ph₃PH⁺) = 2.7,^{15a} and pK_a (CF₃SO₃H) = -4.9, obtained by converting the literature value of 2.6 that is found in acetonitrile^{15b} onto the aqueous scale by means of pK_a (H₂O) = pK_a (MeCN) - 7.5.^{2a}

2a. Complex **3a** (30 mg, 31 μ mol) and variable amounts of Ph₃PH⁺ (13–31 μ mol) were dissolved in 0.5 mL of CD₂Cl₂. Integration of the signals of **2a**, **3a**, Ph₃P, and Ph₃PH⁺ in the inverse-gated decoupled ³¹P NMR spectrum of the solution gave K_{eq} .

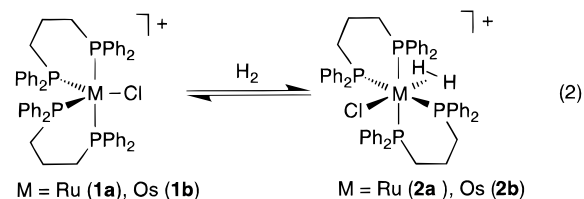
2b. Complex **2b** (20 mg, 17 μ mol) was dissolved in 0.5 mL of CD₂Cl₂ and variable amounts of Et₃N (22–66 μ mol) were added via microsyringe. Integration of the inverse-gated decoupled ³¹P NMR spectrum of the solution gave the concentrations of **2b** and **3b**, from which K_{eq} values were calculated assuming [Et₃NH⁺] = [3b] and [Et₃N] = [Et₃N]₀ - [3b], where [Et₃N]₀ is the total concentration of base added.

4a,b. Complexes **4a** and **4b** (24 μ mol) were dissolved in 0.5 mL of CD₂Cl₂, and Et₃N (7–22 μ mol) was added via microsyringe. K_{eq} values were obtained as described for **2b**.

6b. Complex **6b** (20 mg, 15 μ mol) was dissolved in 0.5 mL of CD₂Cl₂, and CF₃SO₃H (14–24 μ mol) was added via microsyringe. K_{eq} values were obtained from the concentrations of **6b** and **7b**, measured as described above, assuming [CF₃SO₃⁻] = [7b] and [CF₃SO₃H] = [CF₃SO₃H]₀ - [7b], where [CF₃SO₃H]₀ is the total concentration of acid added.

Results

H₂ Addition onto [MCl(dppp)₂]⁺. The reaction of the five-coordinate species [MCl(dppp)₂]⁺ (M = Ru (**1a**), Os (**1b**)) with H₂ (eq 2) was monitored by ¹H and ³¹P NMR spectroscopy. The dihydrogen complex *trans*-[RuCl(η^2 -H₂)(dppp)₂]⁺ (**2a**) is slowly formed when a CD₂Cl₂ solution of **1a** (0.090 mol L⁻¹) is saturated with H₂ (1 atm, 23 °C). The ¹H NMR spectrum of the reaction solution shows a broad signal for the dihydrogen ligand at δ -10.6 and a sharp signal at δ 4.6 for free H₂, while a broad resonance at δ 6.6 appears and gains in intensity in the ³¹P NMR spectrum.



The concentrations of **1a** and **2a**, obtained by integration of the inverse-gated decoupled ³¹P NMR spectra, are constant after 48 h and give a **1a**:**2a** molar ratio of 82:18. Besides **1a** and **2a**, a small amount of [RuH(η^2 -H₂)(dppp)₂]⁺ (**4a**, ca. 1% of starting **1a**) is present during the reaction. Integration of the signals of bound and free dihydrogen in the ¹H NMR spectrum at equilibrium gives a value of 3.3 mmol L⁻¹ for the concentration of free H₂ (corrected for 25% NMR-silent parahydrogen), yielding $K = 0.72 \times 10^2$ mol⁻¹ L (at 23 °C). When the experiment is repeated with an initial H₂ pressure p (H₂) of 2 atm, 37% of **2a** is formed after reaching equilibrium (36 h). The equilibrium concentration of dihydrogen is 8.1 mmol L⁻¹, yielding $K = 0.75 \times 10^2$ mol⁻¹ L (at 23 °C), in good agreement with the value obtained for p (H₂) = 1 atm.

As the relative intensity of free H₂ in solution increases during the time required for reaching the equilibrium position, while no change is observed thereafter, the transfer of dihydrogen from the gas phase to the solution must occur at a rate comparable to that of the reaction of **1** \rightarrow **2**. Thus, no meaningful kinetic information can be derived from these data. However, pre-saturation experiments indicate that the exchange between free and coordinated H₂ is slow compared to their longitudinal relaxation processes, as no magnetization transfer is observed at 22 °C in CD₂Cl₂ by irradiating at the resonance of either free or coordinated H₂.

Complex **1a** does not react in the solid state under 300 atm of H₂ at room temperature during 48 h. However, **2a** is quantitatively formed when a CD₂Cl₂ solution of **1a** (0.090 mol L⁻¹) is kept under 300 atm of H₂ for 24 h. When the H₂ pressure is released to 1 atm, **2a** slowly dissociates H₂ at 22 °C, reaching the same equilibrium position that is obtained when starting from **1a** and saturating the CD₂Cl₂ solution with H₂. Dihydrogen dissociation is inhibited at low temperature: **2a** can be stored for days at -78 °C without changes. Even at 0 °C, **2a** does not decompose significantly over the time needed for the NMR measurements. Thus, **2a** was fully characterized in solution by means of variable-temperature ¹H and ³¹P NMR spectroscopy (Tables 1 and 2).

(15) (a) Allman, T.; Goel, R. G. *Can. J. Chem.* **1982**, *60*, 716. (b) Fujinaga, T.; Sakamoto, I. *J. Electroanal. Chem.* **1977**, *85*, 185.

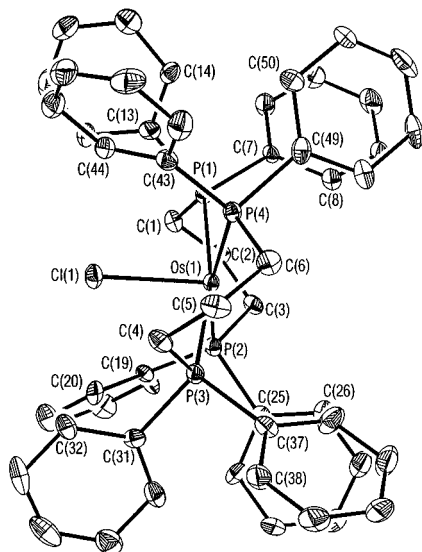


Figure 1. ORTEP view of the $[\text{OsCl}(\eta^2\text{-H}_2)(\text{dppp})_2]^+$ cation **2b**.

The ^1H NMR spectra recorded over the range from -90 to 0°C show that the dihydrogen signal at $\delta -10.6$ broadens as the temperature is lowered. The T_1 of this signal reaches a minimum value of 8.2 ms at -50°C (200 MHz). The deuterio derivative $[\text{RuCl}(\eta^2\text{-HD})(\text{dppp})_2]^+$ (**2a-d₁**) was prepared by reaction of $[\text{RuH}(\text{Cl})(\text{dppp})_2]^{14}$ (**3a**) with the stoichiometric amount of D_2SO_4 in CD_2Cl_2 at 0°C . The low-frequency part of the ^1H NMR spectrum (CD_2Cl_2 , 0°C) of **2a-d₁** consists of a multiplet showing well-resolved couplings both to the D and P nuclei that can be simulated with a $^1J(\text{D},\text{H}) = 24.4\text{ Hz}$ ($^2J(\text{P},\text{H}) = 7.5\text{ Hz}$).

The osmium analog $[\text{OsCl}(\text{dppp})_2]^+$ (**1b**) reacts quantitatively under H_2 (1 atm, 22°C , CH_2Cl_2 solution) within 2 h to give $\text{trans-}[\text{OsCl}(\eta^2\text{-H}_2)(\text{dppp})_2]^+$ (**2b**), which was isolated as its $[\text{PF}_6]^-$ salt. Replacing dihydrogen with argon reverses the reaction, and **1b** is the only species observed by ^{31}P NMR after 24 h. However, **2b** is stable toward loss of H_2 in the solid state for several days at room temperature, even under vacuum. The ^1H NMR signal of the dihydrogen ligand is a broad quintet centered at $\delta -9.97$ [$^2J(\text{P},\text{H}) = 11\text{ Hz}$], which broadens further at low temperature. The T_1 reaches a minimum value of 23.7 ms at -60°C (200 MHz). The deuterio derivative $[\text{OsCl}(\eta^2\text{-HD})(\text{dppp})_2]^+$ (**2b-d₁**) was prepared in various degrees of deuteration either by reacting $[\text{OsHCl}(\text{dppp})]$ (**3b**) with stoichiometric amounts of $\text{F}_3\text{CSO}_3\text{D}$ or by reacting **1b** with HD gas, prepared by reacting LiAlH_4 with D_2O . A low $^1J(\text{D},\text{H})$ value of 11 Hz was obtained by direct observation of the 1:1:1 triplet in the partially relaxed, ^{31}P -decoupled ^1H NMR spectrum. An identical value was obtained by simulation of the ^{31}P -coupled spectrum of **2b-d₁**, using $^2J(\text{P},\text{H}) = 11\text{ Hz}$.

The room temperature ^{31}P NMR spectra of both **2a** and **2b** in CD_2Cl_2 exhibit a broad signal at $\delta 6.6$ and -30.0 , respectively, which splits up and resolves into a multiplet, consistent with an $\text{AA}'\text{XX}'$ system, upon lowering the temperature (Table 1). This indicates that the symmetry of these (formally) octahedral complexes is lowered by some degree of distortion (see below). Interchange of the nonequivalent P atoms is relatively fast at room temperature on the NMR time scale, as indicated by the single, broad signal, while at low temperature the process is frozen out.

X-ray Structure of $[\text{OsCl}(\eta^2\text{-H}_2)(\text{dppp})_2][\text{PF}_6]$. An ORTEP view of the $[\text{OsCl}(\eta^2\text{-H}_2)(\text{dppp})_2]^+$ cation is shown in Figure 1, and selected bond distances and angles are reported in Table 3. The crystal contains discrete $[\text{OsCl}(\eta^2\text{-H}_2)(\text{dppp})_2]^+$ and $[\text{PF}_6]^-$, with normal nonbonded interactions, together with two

CH_2Cl_2 molecules as the solvent of crystallization. The H atoms of the dihydrogen ligand were not located. However, assuming that dihydrogen occupies the sixth coordination position *trans* to Cl, the coordination of the complex cation can be described as distorted octahedral, with *pseudo-C*₂ symmetry about the Os—Cl vector (Figure 1). Both *trans* P—Os—P angles are closed down to values about 168° . The arrangement of the four P atoms is distorted in a tetrahedral fashion from the ideal coplanarity, with P(2) and P(4) pushed away from Cl and P(1) and P(3) bent toward it. The Os atom lies in the P(1)—P(2)—P(3)—P(4) least-squares plane (-0.005 \AA), while P(1), P(2), P(3), and P(4) are symmetrically displaced by 0.237, -0.231 , 0.233, and -0.240 \AA , respectively. The Os—Cl vector approximately bisects the P(1)—Os(1)—P(3) and P(2)—Os(1)—P(4) angles and forms an angle of 2° with the normal to the P(1)—P(2)—P(3)—P(4) least-squares plane. Both chelate rings adopt a twist conformation.

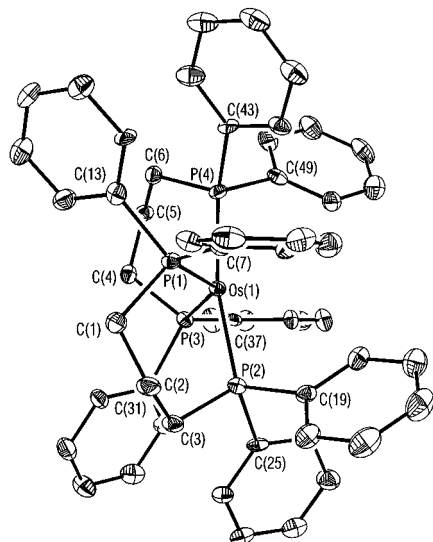
The Os—Cl distance ($2.437(4)\text{ \AA}$) lies at the upper extremity of the range found for six-coordinate Os(II) complexes,¹⁶ suggesting that the $(\eta^2\text{-H}_2)$ ligand exerts a relatively high *trans* influence (see below). The Os—P bond lengths are scattered in a narrow range (Table 3), with an average value of 2.418 \AA . Four phenyl rings form a pocket around the Cl atom, with short separations ($3.30\text{--}3.39\text{ \AA}$) between Cl and the *ortho* phenyl carbons C(18), C(20), C(32), and C(44), while the nonbonded distances between the phenyl rings are normal.

H₂ Addition to $[\text{OsH}(\text{dppp})_2]^+$. The five-coordinate hydride $[\text{RuH}(\text{dppp})_2]^+$ is known to react with H_2 (1 atm) to give $[\text{RuH}(\eta^2\text{-H}_2)(\text{dppp})_2]^+$ (**4a**).¹² A H—H distance of about 0.72 \AA has been estimated on the basis of the $T_1(\text{min})$ of 6 ms (400 MHz, -30°C) and the $^1J(\text{D},\text{H})$ of 32 Hz.^{12b} We find a slightly different $T_1(\text{min})$ of 5.5 ms (CD_2Cl_2 , 200 MHz, 213 K), corresponding to $d(\text{H—H}) = 0.80\text{ \AA}$ (rapidly spinning), while the literature $J(\text{D},\text{H})$ value of 32 Hz gives $d(\text{H—H}) = 0.89\text{ \AA}$.^{9e}

Thus, we attempted the preparation of the osmium analog $[\text{OsH}(\text{dppp})_2]^+$ in order to investigate its reactivity with hydrogen. The six-coordinate $[\text{OsH}(\text{Cl})(\text{dppp})_2]$ (**3b**) was obtained by deprotonation of **2b** with EtONa (see below). Although the CH_2Cl_2 solutions of **3b** turn dark red in the presence of solid $\text{Na}[\text{BPh}_4]$ as a chloride scavenger, suggesting that a five-coordinate species is actually formed, attempts to isolate pure $[\text{OsH}(\text{dppp})_2]^+$ were unsuccessful. However, when the same reaction was repeated under H_2 gas (1 atm), the solution remained colorless and a white complex of composition $[\text{OsH}_3(\text{dppp})_2][\text{BPh}_4]$ (**4b**) was isolated. The same complex cation was obtained by protonation of $[\text{OsH}_2(\text{dppp})_2]$ (**5b**) with $\text{HBF}_4\cdot\text{Et}_2\text{O}$ in CH_2Cl_2 and was isolated as its $[\text{BF}_4]^-$ salt $[\text{OsH}_3(\text{dppp})_2][\text{BF}_4]$.

X-ray Structure of $[\text{OsH}_3(\text{dppp})_2][\text{BPh}_4]$. An ORTEP view of the $[\text{OsH}_3(\text{dppp})_2]^+$ cation is shown in Figure 2, and selected bond distances and angles are reported in Table 4. The crystal contains discrete $[\text{OsH}_3(\text{dppp})_2]^+$ cations and $[\text{BPh}_4]^-$ anions, with normal nonbonded interactions, together with two CH_2Cl_2 molecules as the solvent of crystallization. The positions of the P atoms in the complex cation are in good agreement with a pentagonal bipyramidal structure in which the P(2), P(4) pair approximately occupies the apical positions. The P(1)—P(3) vector is approximately perpendicular to the P(2)—P(4) one (85.2°). It appears reasonable to assume that the equatorial plane is occupied by P(1) and P(3), together with the three undetected hydride ligands. The value of 136.6° found for the P(1)—Os—P(3) angle is not far from the ideal value (144°), as well as the *trans* P(2)—Os—P(4) angle of 169.1° from 180° .

(16) Orpen, A. G.; Brammer, L.; Allen, F. H.; Kennard, O.; Watson, D. G.; Taylor, R. *J. Chem. Soc., Dalton Trans.* **1989**, S1.



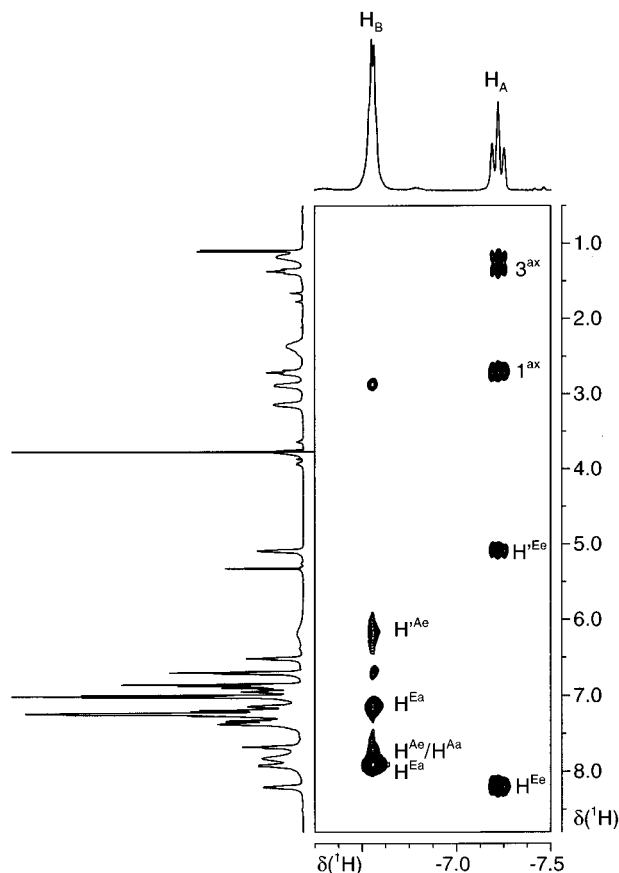
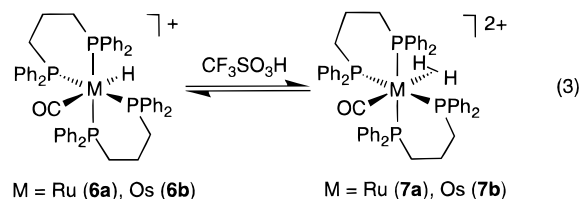


Figure 4. Section of the two-dimensional ROESY spectrum (500 MHz, 193 K, $\tau_{\text{mix}} = 120$ ms) for $[\text{OsH}_3(\text{dppp})_2]^+$ (**4b**) used for locating the two types of hydride ligands.

reaction of **3a,b** with carbon monoxide in a CH_2Cl_2 solution and were precipitated as their $[\text{BPh}_4]^-$ salts by addition of ethanolic $\text{Na}[\text{BPh}_4]$. The osmium analog forms mixtures of *cis*- and *trans*-(**6b**) under these conditions, as already observed for CO addition onto analogous Os(II) five-coordinate species.^{8c} Quantitative conversion to *trans*-(**6b**) is achieved by refluxing the isomer mixture in MeOH for 8 h.

The ruthenium hydrido carbonyl **6a** does not react with $\text{HBF}_4 \cdot \text{Et}_2\text{O}$ ($\text{p}K_a = -2.4$ on the aqueous scale)¹⁸ in anhydrous CD_2Cl_2 , even in the presence of a 5-fold excess of acid. However, **6a** reacts immediately with excess $\text{CF}_3\text{SO}_3\text{H}$ at room temperature. Gas evolution is observed from the solution, apparently arising from the decomposition of an unstable dihydrogen complex (eq 3).



The ^{31}P NMR spectrum indicates that **6a** is converted into a series of products: among the unidentified species, *trans*- $[\text{RuCl}(\text{CO})(\text{dppp})_2]^+$ was observed. However, the dicationic dihydrogen complex $[\text{Ru}(\text{CO})(\eta^2\text{-H}_2)(\text{dppp})_2]^{2+}$ (**7a**) was trapped by protonation of **6a** with excess $\text{CF}_3\text{SO}_3\text{H}$ at -40°C in CD_2Cl_2 and was characterized in solution by low-temperature ^1H and ^{31}P NMR. Reproducible ^1H NMR T_1 data were collected

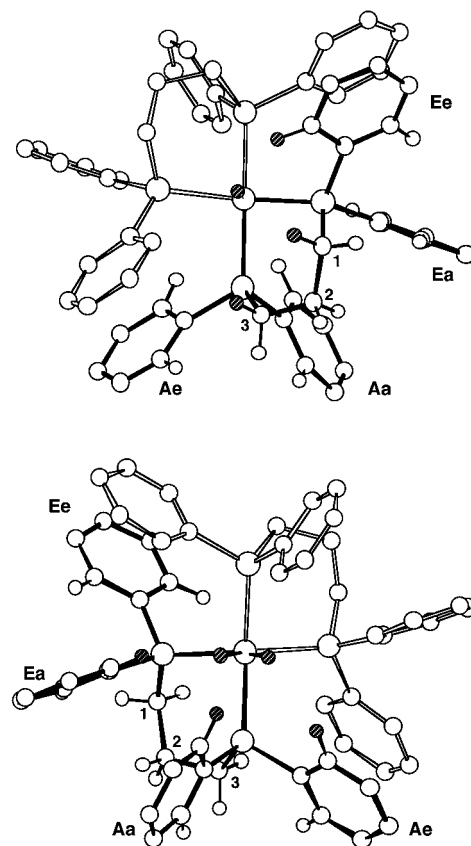
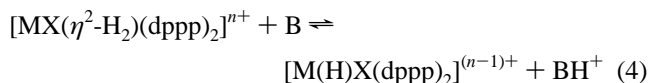


Figure 5. Model showing the locations of the H_A (top) and H_B (bottom) within the pentagonal bipyramidal coordination sphere of Os in $[\text{OsH}_3(\text{dppp})_2]^+$ (**4b**). Hydrides and protons which are spatially close to these are shown in a shaded fashion. For clarity, one of the dppp ligands is contoured.

between -40 and -60°C . The T_1 values reach a minimum of 5.0 ms at -50°C , and a $J(\text{D,H})$ value of 34.2 Hz is found for *trans*- $[\text{Ru}(\text{CO})(\eta^2\text{-DH})(\text{dppp})_2]^{2+}$, obtained by protonation of **6a** with excess $\text{CF}_3\text{SO}_3\text{D}$ (CD_2Cl_2 at -80°C). The single broad signal at δ 7.6 (br s) that is observed in the $^{31}\text{P}\{^1\text{H}\}$ NMR spectrum of **6a** at -30°C resolves into an $\text{AA}'\text{XX}'$ system at low temperature (Table 1).

The osmium derivative **6b** does not react with either $\text{HBF}_4 \cdot \text{Et}_2\text{O}$ (1:1 or 1:3 molar ratio) or a stoichiometric amount of $\text{CF}_3\text{SO}_3\text{H}$ in CD_2Cl_2 solution. However, $[\text{Os}(\text{CO})(\eta^2\text{-H}_2)(\text{dppp})_2]^{2+}$ (**7b**) is quantitatively formed in the presence of excess triflic acid. Complex **7b** is stable at room temperature under both Ar and H_2 but decomposes upon attempts to isolate it in the solid state. The $(\eta^2\text{-H}_2)$ NMR signal is a broad, featureless hump centered at δ -3.0 (CD_2Cl_2 , 200 MHz, 20°C) with a minimum T_1 value of 5.5 ms at -40°C . Protonation of **6b** with 12 equiv of $\text{F}_3\text{CSO}_3\text{D}$ in CD_2Cl_2 gives a $J(\text{D,H})$ value of 32.0 Hz. The room temperature $^{31}\text{P}\{^1\text{H}\}$ NMR spectrum of **7b** shows a single broad signal at δ -29.7 , which resolves into an $\text{AA}'\text{XX}'$ system at low temperature.

Acidity of $[\text{MX}(\eta^2\text{-H}_2)(\text{dppp})_2]^+$. The $\text{p}K_a$ values of the dihydrogen complexes in CD_2Cl_2 were estimated by ^1H and ^{31}P NMR by studying the proton transfer reaction between the dihydrogen complex (or the corresponding hydride) and a suitable secondary internal standard (eq 4):



Investigation involving the stable dihydrogen complexes indicates that these equilibria are established during the time

of mixing; no significant changes are observed by ^1H and ^{31}P NMR after 24 h in the solutions. The aqueous $\text{p}K_{\text{a}}$ value of the dihydrogen complex can be estimated by means of eq 5 from the equilibrium constant K_{eq} of eq 4 and the $\text{p}K_{\text{a}}$ of the base B, extrapolated to the aqueous scale, as suggested by Kristjánssdóttir and Norton:¹⁹

$$\text{p}K_{\text{a}}(\eta^2\text{-H}_2) = \text{p}K_{\text{eq}} + \text{p}K_{\text{a}}(\text{HB}^+) \quad (5)$$

The standard errors observed for K_{eq} 's are small compared to the uncertainty related to the conversion of the $\text{p}K_{\text{a}}$ values of the secondary standards onto the aqueous scale (± 1). In view of the wide $\text{p}K_{\text{a}}$ range observed, bases different than phosphines had to be used in most cases. Protonation studies of chlorohydride **3a** with Ph_3PH^+ in CD_2Cl_2 indicates that the decomposition of the dihydrogen species **2a** is slow compared to the acid–base reaction; detectable amounts of five-coordinate **1a** (3% of starting **3a**) are formed after 5 min. In agreement with the estimated $\text{p}K_{\text{a}}$ value of 4.4 (on the pseudo-aqueous scale), **3a** is not protonated by stoichiometric amounts of Et_3NH^+ . The $\text{p}K_{\text{a}}$ values of **2b** and **4a,b** were obtained by deprotonation with Et_3N (Table 5). As expected on the basis of the measured $\text{p}K_{\text{a}}$ value of 10.3, **4b** is protonated quantitatively by 1 equiv of $[\text{HPPPh}_3]^+$ ($\text{p}K_{\text{a}} = 2.7$).

Although both of the hydrido carbonyl complexes **6a,b** are protonated by excess $\text{CF}_3\text{SO}_3\text{H}$, quantitative NMR measurements for **7a** were not performed due to its instability at room temperature. However, the fact that **7a** is formed quantitatively only in the presence of excess $\text{CF}_3\text{SO}_3\text{H}$ suggests a $\text{p}K_{\text{a}}$ value of *ca.* -6 or lower. In view of the limited reliability of the $\text{p}K_{\text{a}}$ value reported for $\text{CF}_3\text{SO}_3\text{H}$, the $\text{p}K_{\text{a}}$ value of -5.7 for **7b** should be regarded as a rough estimation.

Discussion

NMR Spectroscopy. The available solution NMR spectroscopic data, as well as structural evidence for **2b**, suggest that the dynamic process observed for **2**, **3**, **6**, and **7** is related to the distortions of their pseudo-*trans*-octahedral structure, with two nonequivalent pairs of *trans* P atoms exchanging positions with inversion of the chelate ring conformation. The slow-exchange spectra observed at low temperatures (AA'XX' spin systems, Table 1) indicate that the overall symmetry of these molecules is C_2 , in accordance with the X-ray data of **2b**.

The pentagonal bipyramidal structure of **4b** cannot be discriminated from that of the six-coordinate species **2**, **3**, **6**, and **7** on the basis of the ^{31}P NMR solution spectra, as all show similar temperature dependence and AA'XX' spin systems at low temperature. However, the number of *trans* coupling constants (≥ 100 Hz) observed in the solid state ^{31}P NMR spectrum should be diagnostic of either structure. Unfortunately, the mutually *trans*-oriented P atoms in **2b** are isochronous, which is probably due to the presence of a *pseudo*- C_2 symmetry even in the solid state.

Dihydride vs Dihydrogen Preference. The trend found on going from Ru to Os in the series $[\text{MH}(\text{H}_2)(\text{dppp})_2]^+$, where **4a** is a dihydrogen complex and **4b** a classical trihydride, parallels that found for $[\text{RuH}(\eta^2\text{-H}_2)(\text{dcpe})_2]^+$ vs $[\text{OsH}_3(\text{dcpe})_2]^+$ ^{9b} and for $[\text{RuH}(\text{I})(\eta^2\text{-H}_2)(\text{PCy}_3)_2]^{\text{7a}}$ vs $[\text{Os}(\text{H})_3\text{Cl}(\text{P}^i\text{Pr}_3)_2]^{\text{20}}$. However, the classical nature of the three hydrides in **4b** contradicts the expectations based on both the phosphine

basicity arguments and the structural analogies, as both $[\text{OsH}(\eta^2\text{-H}_2)(\text{dppe})_2]^+$ and $[\text{OsH}(\eta^2\text{-H}_2)(\text{depe})_2]^+$ (depe = 1,2-bis-(diethylphosphino)ethane) are dihydrogen complexes.²¹ A possible explanation may invoke the flexibility of the diphosphine backbone, accounted for by the larger bite angle of dppp, which is close to the “ideal” value of 90° (average values are 89.0 , 86.4 , and 87.6° in **1**,^{8c} **2b**, and **4b**, respectively). This is significantly larger than that for both dppe and depe in $[\text{OsH}(\eta^2\text{-H}_2)(\text{P}-\text{P})_2]^+$, where the average values are 82.2 and 82.9° , respectively.²¹ The flexibility of the diphosphine backbone might allow a pair of *trans* P atoms to bend away from the octahedral geometry toward a seven-coordinate trihydride structure.²² Accordingly, the ligand 1,1-bis(diphenylphosphino)-ferrocene (dppf) favors the formation of the classical trihydride $[\text{RuH}_3(\text{dppf})_2]^+$, in which the dppf ligand adopts an average bite angle of 106.4° .²³ Calculations taking into account both the steric and electronic energies in $[\text{RuH}_3(\text{diop})_2]^+$ have shown that the next low-energy isomer (after the absolute minimum relative to *trans*- $[\text{RuH}(\eta^2\text{-H}_2)(\text{diop})]^+$) is a classical trihydride structurally related to **4b** and $[\text{RuH}_3(\text{dppf})_2]^+$.²⁴

Dihydrogen complexes are observed in the osmium series when X is a weaker σ -donor than hydride, as the electron density at the metal is lowered. Thus, a change from classical hydrides to an elongated dihydrogen complex is observed on going from hydride to Cl, as in $[\text{M}(\text{H})_3(\text{dppe})_2]$ ($\text{M} = \text{Tc}, ^{9c} \text{Re}^{21a,25}$) vs $[\text{MCl}(\eta^2\text{-H}_2)(\text{dppe})_2]^+$ ($\text{M} = \text{Tc}, ^{9c} \text{Re}^{26}$) and in $[\text{ReH}_3(\text{PMePh}_2)_4]$ vs $[\text{ReCl}(\eta^2\text{-H}_2)(\text{PMePh}_2)_4]^+$.²⁷ When X is a strong π -acceptor, such as CO, the d^n (M) orbitals are further depleted and “short” dihydrogen ligands are observed for both metals (see below).

H–H Distances in the $(\eta^2\text{-H}_2)$ Complexes. The T_1 (min) values of the dihydrogen ligands and the $^1J(\text{D},\text{H})$ values in the analogous deuterated complexes are summarized in Table 2. Equation 6,^{9c} recently developed from the correlation between the $J(\text{D},\text{H})$ and $d(\text{H}-\text{H})$ values observed earlier,^{2b} gives values in substantial agreement with those from the procedure of Hamilton and Crabtree that was based on T_1 (min) values²⁸ and avoids the choice between different models (“rapid spinning” or “slow rotation”). The $d(\text{H}-\text{H})$ values in Table 2 span nearly the whole range known. The $d(\text{H}-\text{H})$ value of 1.0 Å calculated for **2a** ($J(\text{D},\text{H}) = 24$ Hz) is near that of 1.10 Å found by neutron diffraction for $[\text{Ru}(\text{H}\cdots\text{H})(\text{C}_5\text{Me}_5)(\text{dppm})]$ ($J(\text{D},\text{H}) = 21$ Hz).²⁹ For **2b**, the $J(\text{D},\text{H})$ and $d(\text{H}-\text{H})$ values of 11 Hz and 1.2 Å are similar to those of *trans*- $[\text{Os}(\eta^1\text{-O}_2\text{CCH}_3)(\eta^2\text{-H}_2)(\text{en})_2]^+$ ($J(\text{D},\text{H}) = 9$ Hz, $d(\text{H}-\text{H}) = 1.34$ Å by neutron diffraction), which lie at the low extremity of the range found for dihydrogen complexes.^{11c}

$$d(\text{H}-\text{H}) = -0.0167J(\text{D},\text{H}) + 1.42 \quad (6)$$

- (19) Kristjánssdóttir, S. S.; Norton, J. R. In *Transition Metal Hydrides*; Dedieu, A., Ed.; VCH: Weinheim, FRG, 1992; Chapter 9, pp 324–334.
(20) Gusev, D. G.; Kuhlmann, R.; Sini, G.; Eisenstein, O.; Caulton, K. G. *J. Am. Chem. Soc.* **1994**, *116*, 2685.

- (21) (a) Earl, K. A.; Jia, G.; Maltby, P. A.; Morris, R. H. *J. Am. Chem. Soc.* **1991**, *113*, 3027. (b) Farrar, D. H.; Maltby, P. A.; Morris, R. H. *Acta Cryst. (C)*, **1992**, *48*, 28. Earl, K. A.; (c) Morris, R. H.; Sawyer, J. F. *Acta Crystallogr., Sect. C* **1989**, *45*, 1137.
(22) Van Der Sluys, L. S.; Eckert, J.; Eisenstein, O.; Hall, J. H.; Huffman, J. C.; Jackson, S. A.; Koetzle, T. F.; Kubas, G. J.; Vergamini, P. J.; Caulton, K. G. *J. Am. Chem. Soc.* **1990**, *112*, 4831.
(23) Saburi, M.; Aoyagi, K.; Kodama, T.; Takahashi, T.; Uchida, T. *Chem. Lett.* **1990**, 1909.
(24) Maseras, F.; Koga, N.; Morokuma, K. *Organometallics* **1994**, *13*, 4008.
(25) Albano, V. G.; Bellon, P. L. *J. Organomet. Chem.* **1972**, *37*, 151.
(26) Kohli, M.; Lewis, D. J.; Luck, R. L.; Silverton, J. V.; Sylla, K. *Inorg. Chem.* **1994**, *33*, 879.
(27) (a) Cotton, F. A.; Luck, R. L. *Inorg. Chem.* **1989**, *28*, 2181. (b) *Ibid.* **1991**, *30*, 767.
(28) Hamilton, D. G.; Crabtree, R. H. *J. Am. Chem. Soc.* **1988**, *110*, 4126.
(29) Bautista, M. T.; Earl, K. A.; Maltby, P. A.; Morris, R. H.; Schweitzer, C. T.; Sella, A. *J. Am. Chem. Soc.* **1988**, *110*, 7031.
(29) Klooster, W. T.; Koetzle, T. F.; Jia, G.; Fong, T. P.; Morris, R. H.; Albinati, A. *J. Am. Chem. Soc.* **1994**, *116*, 7677 and references therein.

The effects of X on $d(\text{H}-\text{H})$ can be discussed qualitatively in terms of the $\sigma(\eta^2\text{-H}_2) \rightarrow d^n(\text{M})$ and $d^n(\text{M}) \rightarrow \sigma^*(\eta^2\text{-H}_2)$ bonding components. The high *trans* influence of hydride weakens the former and, synergistically, also the latter component. In the case of CO, the π -acid ligand not only exerts a high *trans* influence, but also stabilizes the $d^n(\text{M})$ orbitals and further reduces their overlap with the $\sigma^*(\eta^2\text{-H}_2)$ orbital. Both effects strengthen the H–H bonding and reduce the $\text{M}(\eta^2\text{-H}_2)$ interaction, giving rise to $(\eta^2\text{-H}_2)$ complexes with short H–H distances. Density functional studies of $J(\text{D},\text{H})$ predict a short $d(\text{H}-\text{H})$ in *trans*- $[\text{OsX}(\eta^2\text{-H}_2)(\text{NH}_3)_4]^{n+}$ when X is a π -acid (CN^-), but the experimental value is not known.³⁰

When X is a π -donor, the low *trans* influence of Cl^- favors the $\sigma(\eta^2\text{-H}_2) \rightarrow d^n(\text{M})$ donation, while the four-electron destabilization between the filled d_π orbital of the metal and the filled p_π orbital of the halide³¹ results in a higher energy of the d^n orbitals and increased $d_\pi(\text{M}) \rightarrow \sigma^*(\eta^2\text{-H}_2)$ back-bonding. Both effects weaken the H–H bond and increase the $\text{M}(\eta^2\text{-H}_2)$ interaction, and elongated dihydrogen complexes are formed. Interestingly, in **2b**, two *trans* P atoms are bent away from the dihydrogen ligand, like in $[\text{Re}(\text{Cl})(\eta^2\text{-H}_2)(\text{PMePh}_2)_4]$.^{27b} This structural feature is known to enhance $d_\pi(\text{M}) \rightarrow \sigma^*(\eta^2\text{-H}_2)$ back-bonding.^{22,24} Independent evidence for dihydrogen being a π -acceptor^{11c,32} comes from the long Os–Cl distance observed in **2b**.

Effect of X on the Stability of the $(\eta^2\text{-H}_2)$ Complexes. Cationic Ru and Os dihydrogen complexes containing CO as a π -acid coligand are relatively rare.^{2a,d,f,4a} The same can be said for dicationic dihydrogen complexes.^{2f,11,33} Morris' additive ligand approach allows one to predict the instability of **7a**, a dicationic dihydrogen complex containing a strong π -acid.^{2a} Also, the protonation of species of the type $[\text{MH}_2(\text{CO})\text{L}_3]$ (M = Ru, Os; L = P-donor ligand) with strong acids does not yield stable dihydrogen complexes.³⁴ Thus, it is rather surprising that **7b** is stable under ambient conditions. Although a *trans* arrangement of dihydrogen and carbonyl ligands is common in neutral d^6 Mo and W complexes¹ and is documented in cationic rhenium(I) complexes,⁵ it is still unprecedented, to the best of our knowledge, in dicationic species of Ru and Os. In addition to several neutral (dihydrogen) osmium carbonyls,^{1,35} a *cis* arrangement of CO and $\eta^2\text{-H}_2$ ligands has been found for $[\text{Os}(\text{CO})(\eta^2\text{-H}_2)(\text{PPh}_3)_2(2\text{-pyridinethiol})]^+$ and $[\text{Os}(\text{CO})(\eta^2\text{-H}_2)(\text{PPh}_3)_2\text{L}_2]^{2+}$ (L = $1/2\text{bpy}$ or PPh_3).^{2d,f}

The effects of the ancillary ligand X on the σ and π bonding components account for the trend in the stability of the $\text{M}(\eta^2\text{-H}_2)$ bond in the ruthenium complexes, which increases in the order $\text{CO} < \text{Cl} < \text{H}$. The lower stability with CO than with H reflects the weakening of the $d_\pi(\text{M}) \rightarrow \sigma^*(\eta^2\text{-H}_2)$ bonding component due to the π -acid. Dissociation of dihydrogen from **7a** gives a highly reactive 16-electron species: the $[\text{Ru}(\text{CO})-$

$(\text{dppp})_2]^{2+}$ fragment is a powerful Lewis acid that abstracts Cl from CD_2Cl_2 . In the case of Os, the dihydrogen complex **B** is relatively stable, probably because the metal is more electron rich than Ru and the high-energy 16-electron fragment **A** resulting from H_2 dissociation is not stabilized by dimerization or agostic interactions.

The intermediate stability of the chloro derivatives **2a,b** is not obvious at first, as the elongation of the dihydrogen ligand is indicative of a strong $\text{M}(\eta^2\text{-H}_2)$ bond. However, the K_{eq} data available for **2a** show that *longer* H–H bonds do not necessarily go along with increased *thermodynamic stability*. This is probably due to the stabilization of the 16-electron fragment by the π -donor. Accordingly, the presence of one or more π -donors in an octahedral, nonclassical polyhydride complex of a d^6 metal ion is known to induce dissociation of one dihydrogen ligand by the combined effects of the four-electron destabilization mentioned above³¹ and the stabilization of the 16-electron fragment by means of $\text{Cl} \rightarrow \text{M} \pi$ -donation.⁶ Thus, if fragment **A** is a π -stabilized five-coordinate complex, the position of equilibrium *a* in eq 1 depends on the effectiveness of the π -donation from X to the metal. As π -stabilized unsaturated compounds have been used as hydrogenation catalyst precursors, the reactivity of such species toward dihydrogen is a theme of particular interest.

Complex **1a** is known to be a Y-shaped complex, which is not stabilized by any agostic interaction; the shortest Ru–C(phenyl) nonbonded contacts are 3.42 and 3.51 Å.^{8c} The Ru–Cl bond length is expected to be diagnostic of π -bonding between the 16-electron fragment and the π -donor chloride.^{6a} Indeed, the Ru–Cl distance in **1a** (2.371(5) Å) is significantly shorter than the average of 2.435(16) Å found for 34 values in 17 six-coordinate complexes of the type *cis*- or *trans*- $[\text{RuCl}_2\text{L}_4]$ (L = phosphine ligand), as retrieved from the Cambridge Structural Database after discarding eight values of four complexes of the type *cis*- $[\text{RuCl}_2(\text{PR}_3)_4]$ (R = alkyl). The Ru–Cl distance is shorter in **1a** than in $[\text{RuCl}(\text{dcpe})_2]^+$ and $[\text{RuCl}(\text{dppe})_2]^+$ (2.386(3) and 2.395(2) Å, respectively). This suggests that if it is accepted that the 16-electron species $[\text{RuCl}(\text{P}-\text{P})_2]^+$ (P–P = dppp, dcpe, dppe) are π -stabilized to some extent, then this effect is largest in **1a**. Accordingly, among the complexes of the type $[\text{RuCl}(\text{P}-\text{P})_2]^+$, only **1a** does not react quantitatively with H_2 under ambient conditions.

As the presence of a π -donor is responsible for both the elongation of the H–H bond and the stabilization of the five-coordinate dissociation product **A**, the position of equilibrium *a* in eq 2 ultimately depends on the balance between these two effects. For **1a**, the stabilization of the five-coordinate **A** appears to overrun the effect of the increased interaction between the metal center and the dihydrogen ligand, while in **1b**, the contrary seems to be the case. Finally, the increasing stability on going from Ru to Os, a general feature of dihydrogen complexes, is thought to be related to the increase in the strength of the $\text{M}(\eta^2\text{-H}_2)$ bonding on going down the group.³⁶

Effect of X on the Acidity. The complexes of the type *trans*- $[\text{MX}(\eta^2\text{-H}_2)(\text{dppp})_2]^+$ (M = Ru, Os; X = H, Cl, CO) allow one to monitor the effect of X on the acidity. Admittedly, the comparison of the $\text{p}K_a$ data for the sequence X = H, Cl, CO is complicated by the fact that **4b** is a classical trihydride. For the Ru complexes, the acidity of the dihydrogen ligand increases in the sequence $\text{H} < \text{Cl} < \text{CO}$, with a trend similar to that in the series $[\text{Os}(\text{X})(\eta^2\text{-H}_2)(\text{dppe})_2]^{n+}$ (X = H, CH_3CN , Cl, Br).^{2e} The most striking feature is the wide range of $\text{p}K_a$ values, spanning 18 $\text{p}K_a$ units! This can be qualitatively explained on

- (30) Backsay, G. B.; Bytheway, I.; Hush, N. S. *J. Am. Chem. Soc.* **1996**, *118*, 3753.
- (31) Albinati, A.; Bakhmutov, V. I.; Caulton, K. G.; Clot, E.; Eckert, J.; Eisenstein, O.; Gusev, D. G.; Grushin, V. V.; Hauger, B. E.; Klooster, W. T.; Koetzle, T. F.; McMullan, R. K.; O'Loughlin, T. J.; Pélissier, M.; Ricci, J. S.; Sigalas, M. P.; Vymenits, A. B. *J. Am. Chem. Soc.* **1993**, *115*, 7300.
- (32) Morris, R. H.; Schlaf, M. *Inorg. Chem.* **1994**, *33*, 1725.
- (33) Smith, K. T.; Tilset, M.; Kuhlmann, R.; Caulton, K. G. *J. Am. Chem. Soc.* **1995**, *117*, 9473.
- (34) (a) Siedle, A. R.; Newmark, R. A.; Pignolet, L. H. *Inorg. Chem.* **1986**, *25*, 3412. (b) Blosser, P. W.; Gallucci, J. C.; Wojcicki, A. *Inorg. Chem.* **1992**, *31*, 2376.
- (35) (a) Gusev, D. G.; Vymenits, A. B.; Bakhmutov, V. I. *Inorg. Chem.* **1992**, *31*, 1. (b) Buil, M. L.; Esteruelas, M. A.; Lahoz, F. J.; Oñate, E.; Oro, L. A. *J. Am. Chem. Soc.* **1995**, *117*, 3619. (c) Esteruelas, M. A.; Lahoz, F. J.; Oñate, E.; Oro, L. A.; Valero, C.; Zeier, B. *J. Am. Chem. Soc.* **1995**, *117*, 7935 and references therein.

- (36) Cappellani, E. P.; Drouin, S. D.; Jia, G.; Maltby, P. A.; Morris, R. H.; Schweitzer, C. T. *J. Am. Chem. Soc.* **1994**, *116*, 3375.

the basis of the effect of X on the relative energies of **A**, **B**, and **C** in eq 1.

The low acidity of $[\text{MH}(\eta^2\text{-H}_2)\text{L}_4]^+$ results from the combination of the strong H–H bond of **B** discussed above and the energetically unfavorable *trans* arrangement of the hydride ligands in **C**. By contrast, a π -accepting X stabilizes **C** relative to both **B** and **A**. This is due to the competition for the d^n (M) electrons between X and dihydrogen in **B** and to the electron-deficient nature of **A**. The result is that **B** is a strong acid when $\text{X} = \text{CO}$. The effect of CO on the acidity of dihydrogen complexes is not restricted to *trans* geometries, as both $[\text{Os}(\text{CO})(\eta^2\text{-H}_2)(\text{PPh}_3)_2(2\text{-pyridinethiol})]^+$ and $[\text{Os}(\text{CO})(\eta^2\text{-H}_2)(\text{bpy})(\text{PPh}_3)_2]^{2+}$ are highly acidic.^{2d,f}

The presence of a π -donor *trans* to dihydrogen increases the $d_\pi(\text{M}) \rightarrow \sigma^*(\eta^2\text{-H}_2)$ back bonding and stabilizes the dihydrogen complex **B** relative to the six-coordinate hydride **C**, as in the latter no π -acid relieves the four-electron $d_\pi(\text{M})\text{--}p_\pi(\text{Cl})$ destabilization. However, the energy of **C** is much lower with $\text{X} = \text{Cl}$ than with H, in view of the energetically favorable *trans* arrangement of Cl and hydride. The result is a $\text{p}K_a$ value for **2a** intermediate between those of **4a** and **7a**. Loss of the dihydrogen ligand according to (a) in eq 1 is also favored due to the formation of a π -stabilized five-coordinate complex. Finally, the decreasing acidity on going from **2a** to **2b** probably reflects an increase in ΔH_{BDE} for the $\text{M}(\eta^2\text{-H}_2)$ bonding going down the group.^{2a,19,36}

Concluding Remarks

The properties of the dihydrogen complexes *trans*- $[\text{MX}(\eta^2\text{-H}_2)(\text{dppp})_2]^+$ can be tuned over the whole $d(\text{H}\text{--}\text{H})$ and $\text{p}K_a$ ranges yet observed, taking advantage of the sensitivity of the H–H distance and Brønsted acidity to the electronic structure of the ancillary ligand X. The rational exploitation of this phenomenon may allow for the synthesis of novel five-coordinate species of the type $[\text{MX}(\text{dppp})_2]^+$ and of the corresponding dihydrogen complexes *trans*- $[\text{MX}(\eta^2\text{-H}_2)\text{L}_4]^+$ for the efficient heterolytic activation of dihydrogen. Also, the present data suggest that the $\eta^2\text{-H}_2$ *vs* dihydride preference is driven by the steric properties of the diphosphine ligand as well as by its basicity.

Acknowledgment. The authors are grateful to Professor R. H. Morris for helpful discussion and for making available his results prior to publication. E.R. gratefully acknowledges the Regione Autonoma Friuli-Venezia Giulia for a fellowship.

Supporting Information Available: Tables of atomic coordinates and equivalent isotropic displacement coefficients, anisotropic thermal parameters, full listings of bond distances and angles, and H atom coordinates (13 pages). Ordering information is given on any current masthead page.

IC9605579